Uchida, T., Song, Y., Mitsuhata, Y., Lee, S. K., Application of 3D magnetotelluric investigation for geothermal exploration – Examples in Japan and Korea. International Symposium on the Fusion Technology of Geosystem Engineering, Rock Engineering and Geophysical Exploration
Seoul, Korea, Nov. 18-19, 2003

Application of 3D magnetotelluric investigation for geothermal exploration – Examples in Japan and Korea

Toshihiro Uchida[1], Yoonho Song[2], Yuji Mitsuhata[1], Seong Kon Lee[2]
[1]Geological Survey of Japan, AIST, Tsukuba, Japan
[2]Korea Institute of Geoscience and Mineral Resources, Daejeon, Korea

Abstract: A three-dimensional (3D) inversion technique has been developed for interpretation of magnetotelluric (MT) data. The inversion method is based on the linearized least-squares (Gauss-Newton) method with smoothness regularization. In addition to the underground 3D resistivity distribution, static shifts are also treated as unknown parameters in the inversion. The forward modeling is by the staggered-grid finite difference method. A Bayesian criterion ABIC is applied to search the optimum trade-off among the minimization of the data misfit, model roughness and static shifts. The method has been applied to several MT datasets obtained at geothermal fields in Japan and other Asian countries. In this paper, two examples will be discussed: one is the data at the Ogiri geothermal area, southwestern Japan, and the other is at the Pohang low-enthalpy geothermal field, southeastern Korea. The inversion of the Ogiri data has been performed stably, resulting in a good fitting between the observed and computed apparent resistivities and phases. The recovered 3D resistivity structure is generally similar to the two-dimensional (2D) inversion models, although the deeper portion of the 3D model seems to be more realistic than that of the 2D model. The 3D model is also in a good agreement with the geological model of the geothermal reservoirs. 3D interpretation of the Pohang MT data is still preliminary. Although the fitting to the observed data is very good, the preliminary 3D model is not reliable enough because the station coverage is not sufficient for a 3D inversion.

1. Introduction

The MT method is still a major geophysical tool in geothermal exploration. Particularly, at an early stage of exploration, a resistivity model is key information to decide the location of pilot and production drillings. In such tasks, 2D inversion has been a standard technique for MT data interpretation in the past decade.

We often utilize TM-mode data for 2D interpretation of MT data in geothermal fields. It is mainly because we usually cannot achieve a good fitting for the TE-mode data by 2D inversion unless the subsurface structure is almost 2D. The TM-mode data can be easily explained by a 2D model, even if the real structure is 3D-like. However, the resultant 2D model may be unrealistic or contain false anomalies, although the final misfit of the TM-mode data can become small. Particularly, the resistivity model of deeper parts of the reservoir structure is often ambiguous.

To overcome such problems, 3D MT inversion techniques have been intensively studied in the past several years (e.g., Sasaki, 1999; Mackie et al., 2001). Sasaki (1999, 2001) developed a 3D MT inversion technique and tested it with several synthetic datasets. Sasaki (2001) proposed to estimate static shifts simultaneously by the inversion. Uchida et al. (2002) applied the method to the MT data obtained in a geothermal field in Indonesia. The resultant 3D models properly indicated the general features of the reservoir structure.

In this paper the inversion technique is applied to a large volume MT dataset obtained in the Ogiri geothermal area, southwestern Japan, and a smaller volume data obtained in the Pohang geothermal field, southeastern Korea. The former dataset was obtained aiming at a 3D study with a grid-like station arrangement, while the latter data was obtained for 2D inversion only on three survey lines. For this work, a function to choose the optimum regularization with regard to the roughness and static shift minimization has been added to the 3D inversion technique so that a stable convergence could be attained almost for any MT dataset that is contaminated by various noises and static shifts.

2. 3D Inversion Technique

The 3D inversion scheme used in this work is based on the linearized iterative least-squares (Gauss-Newton) method with smoothness regularization (Sasaki, 1999). The forward modeling for a given arbitrary 3D earth is by the staggered grid finite difference method. For the modeling, the solution region, including both air and earth, is

discretized into rectangular cells. The area of the solution region is wide enough as compared with the skin depth of the lowest frequency used for the inversion. Outside of the solution region is a layered earth as a background medium. The topography is not incorporated. The electric field is first solved in frequency domain by the finite difference method. Then, the magnetic field is computed from the obtained electric field.

The Jacobian matrix consisting of partial derivatives (sensitivities) of MT responses with respect to block resistivities in the 3D model should be evaluated from an estimated model at each iteration step in the usual iterative Gauss-Newton procedure. However, in this work, to save the computation time, the full sensitivities of the MT responses are computed at only a limited number of iterations; practically only at two iterations, for example, at the 3rd and 6th iterations. A Jacobian matrix computed from a homogeneous earth is used at the 1st and 2nd iterations. After the 3rd iteration, except the 6th iteration, the Broyden method is applied to updating the Jacobian matrix. These approximations may prevent us from reaching perfect resolution and reliability of the inverted 3D model. However, as described in the later sections, the results obtained by this method are acceptable in terms of the data misfit and stableness of the inversion.

In addition to block resistivities of the 3D model, static shifts are also treated as unknowns in the inversion (Sasaki, 2001). A static shift is caused by shallow small inhomogeneities, and observed as a frequency-independent bias on apparent resistivity values, without changes in phase values. The amount of the shift is completely arbitrary and impossible to estimate from the observed apparent resistivity data. In this inversion, Gaussian-distributed static shifts are assumed, and a regularization that the L-2 norm of static shifts is close to zero is applied.

To stabilize the model correction at each iteration step, smoothness regularization is adopted. The objective function U to be minimized in the inversion is defined as,

$$U = \left\| \mathbf{W}\left[\mathbf{d} - F(\mathbf{m}) - \mathbf{G}\mathbf{s}\right] \right\|^2 + \alpha^2 \left(\left\| \mathbf{C}\mathbf{m} \right\|^2 + \beta^2 \left\| \mathbf{s} \right\|^2 \right), \quad (1)$$

where $\mathbf{W}$ is the weight defined from observation errors, $\mathbf{d}$ is the observed data (apparent resistivity and phase), $\mathbf{m}$ is a 3D resistivity model, F is a non-linear function that works on the model $\mathbf{m}$ to produce MT responses, $\mathbf{C}$ is a roughening matrix, $\mathbf{s}$ is the static shift, and $\mathbf{G}$ is a matrix that relates static shifts and the MT responses. The first term of the right-hand side is for the misfit minimization and second term is for roughness and static-shift minimization. α and β are trade-off parameters for roughness minimization and static-shift minimization, respectively, with regard to the misfit minimization.

An optimum regularization for the smoothness, α, and the static shift, β, is searched based on the ABIC minimization method at each iteration (Uchida, 1993). To reduce the search procedure, the optimum smoothness is searched every iteration except every 3rd iteration, while the optimum static shift is searched only every 3rd iteration, both by minimizing a Bayesian criterion ABIC. The initial β is set as 1 or 2 so that the regularization of the static shift minimization would be a similar level to that of the roughness minimization at the first two iterations.

3. Interpretation of Ogiri MT Data

Ogiri geothermal area

The Ogiri geothermal area is located in a southern part of Kyushu Island, southwestern Japan (Fig. 1). A 30-MWe geothermal power plant has been in operation by Nittetsu Kagoshima Geothermal Co., Ltd. (NKG) since 1996. The Shiramizugoe field, neighboring to Ogiri, is estimated to be a promising filed for future exploitation. The survey area is situated on a highland whose elevation is from 700 m to 900 m. The area is underlain by Quaternary volcanic rocks of a thickness of more than 2 km. Below this layer is a Mesozoic metamorphic formation that forms a basement layer of this region. Three faults in an ENE-WSW direction have been identified in the survey area: Sakkogawa, Ginyu and Shiramizugoe from north to south. The major production zone of the Ogiri geothermal reservoir is associated with the Ginyu Fault (Goko, 2000). A new geothermal resource is under exploration by targeting the Shiramizugoe Fault. The geothermal reservoir in this area is distributed in the Quaternary volcanic layers that are mostly consisting of tuff and lava erupted from young volcanoes to the south and east of the area. The heat source of the current reservoir system is estimated to be the Kirishima volcano, which is an active volcano, a few kilometers to the east of the survey area.

The New Energy and Industrial Technology Development Organization (NEDO), NKG, and Geological Survey of Japan (GSJ) have conducted magnetotelluric surveys since 1996 over the Ogiri and Shiramizugoe geothermal fields at several stages. Intensive surveys were conducted by NEDO at Ogiri in 1999 for precise reservoir monitoring and at Shiramizugoe in 2000 for exploration of a new geothermal field. More than ten survey lines were set in the NW-SE direction so that they were perpendicular to the geologic strike, which was the direction of the faults.

The spacing of the survey lines was 250 - 500 m. MT stations were basically arranged on the survey lines with an interval of 150 - 300 m. The MT stations therefore covered the two geothermal fields with a dense grid-like array, which was suitable for a 3D interpretation. The remote reference analysis was applied to all the data with a reference site that was located approximately 40 km south from the survey area.

3D interpretation

For the 3D inversion, the MT impedance was rotated to the direction of the survey lines. Directions of x- and y-axes were 150 and 60 degrees clockwise from north, respectively. The off-diagonal components of the MT impedance (apparent resistivity and phase) were used as the observed data. The numbers of MT stations and frequencies used for the inversion were 158 and 11 (from 0.0703 Hz to 72 Hz), respectively. Very noisy data whose observation error was greater than 200% were omitted before the inversion. Total number of observed data was 6912. The noise floor was assumed as 1%.

The cell size of the finite difference mesh in the interpreted zone (shown in Fig. 1) was 150 m horizontally. The number of cells in the whole mesh was 68, 62 and 33 in x, y and z directions, respectively. Several cells were grouped into a resistivity block whose resistivity was dealt as an unknown parameter. The number of blocks in x, y and z directions was 18, 15 and 14, respectively. Therefore, the total number of resistivity blocks was 3780. The initial model was a homogeneous half space, whose resistivity was the average of the whole apparent resistivity data, which was 21 ohm-m.

Fig. 2 shows depth-slice sections of the final 3D model at the 8th iteration. The normalized RMS misfit is 10.79, and the average of the estimated static shifts is 0.744 in the natural logarithmic domain. Fig. 3 shows the observed and calculated apparent resistivities and phases for the stations on Lines A and B. Fitting of the data is generally fine. Fitting for other stations is similar to that of Fig. 3. The splitting of the two apparent resistivity curves below 1 Hz is not so large, but values of ρa-yx are greater than ρa-xy at most of the sites in this area. This feature indicates that these stations are located on a high-resistivity zone whose strike is close to x-axis. It is consistent with the resistivity structure deeper than 1.5 km in the 3D model in Fig. 2.

The average of the estimated static shifts, 0.744, is relatively large. It is probably because of local topographic effects or complex changes of the surface resistivity. We can recognize large splits between the two apparent resistivity curves at higher frequencies at many sites. Also, there are large gaps in apparent resistivity between several neighboring sites. These shifts are well estimated by the inversion. Stations from 350 to 353 on Line-B are close to the production wells and the power plant. Therefore, the data quality of these stations is not good.

Resistivity structure of this area is characterized by a three-layer model: resistive first layer, conductive second layer and resistive third layer (Fig. 2). Resistivity distribution of the shallow layers (less than a depth of 300 m) has a clear contrast between the high-resistivity zone in the northern half of the survey area and the low-resistivity zone in the southern half (Fig. 2). At the mid depth, say from 400 m to 800 m, the whole area shows low resistivity. Then below a depth of about 800 m, high-resistivity anomalies are recognized at the center of the area, and they occupy the whole area at a depth of 2 km.

On the sections shallower than the 400 m depth, we can recognize the low-resistivity anomalies associated with the two faults, Ginyu and Shiramizugoe. As mentioned above, the low-resistivity anomaly is very wide around the Shiramizugoe Fault at the shallow depth. These can be interpreted as a zone of intensive clay alteration. The shallow high-resistivity zone in the northern side of the Sakkogawa Fault seems to be due to unaltered young lava layer At a depth of about 1000 m, the resistivity structure is not consistent with the surface faults. The strike of this resistive anomaly is approximately NW-SE. We interpret the higher resistivity zones at the center of the survey area indicate the top of the geothermal reservoirs.

Fig. 4 compare vertical sections of the 3D model along Lines A and B with 2D inversion results of TM-mode data. For Line-A, 2D and 3D models are very consistent with each other over the whole sections (Fig. 4a). For Line-B, the upper boundary of the low-resistivity layer is similar between the 2D and 3D models. However, the lower boundary of the low-resistivity layer is different (Fig. 4b). The 3D model shows a smoother boundary, while the 2D model shows that the low-resistivity anomaly continues to deep at the Sakkogawa and Ginyu Faults and at the Shiramizugoe Fault. These may be false anomalies caused by TM-mode data that is insensitive to deep structure In this sense, the 3D model is more realistic than the 2D models.

Fig. 5 shows a simplified geologic section estimated from the drilling data in the Ogiri geothermal field (NEDO, 2000). The Mesozoic basement layer is situated at a depth of about 2.5 km. Above it are Quaternary volcanic layers The Ogiri geothermal reservoir is associated with the Ginyu Fault and located in the Quaternary volcanic layers. The temperature contours of 200 and 225 degrees Celsius indicate high-temperature anomalies beneath the Ginyu and Shiramizugoe Faults. The clay cap, in which low-temperature clay mineral such as smectite is dominant, is dis-

tributed in a zone whose temperature is below 200 degrees Celsius. Shapes of the lower boundary of the clay cap and the contour of 200 degrees Celsius are not only consistent with each other, but also consistent with the boundary between the conductive second layer and the resistive third layer in the vertical resistivity sections of the 3D model (Fig. 4). The Ogiri production zone is located in the high-resistivity and high-temperature anomaly in the left-hande side (x = 2 km in Fig. 4) of the sections of the 3D model. A new production zone of the Shiramizugoe reservoir has been found by NEDO's pilot drillings targeting the high-resistivity and high-temperature anomaly in the right hand side (x = 4 km).

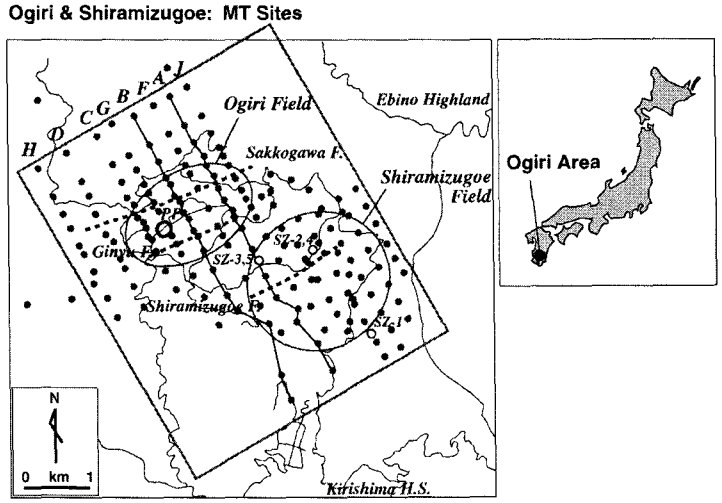

Fig. 1. MT stations over the Ogiri and Shiramizugoe geothermal fields, southwestern Japan. Dots are MT stations, small open circles are pilot drillings, the large open circle with the letters PP is the Ogiri power plant, large ovals indicate centers of two geothermal fields, dashed lines are estimated faults, and thin solid lines are local roads. Letters A-H indicate names of the NW-SE survey lines. Lines A and B are shown with thick solid lines. The large rectangle indicates the region of 3D interpretation.

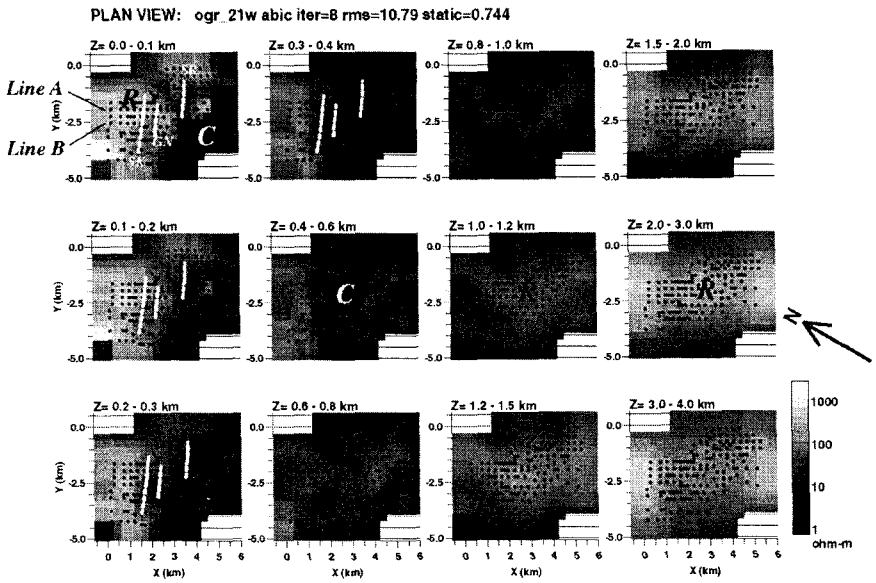

Fig. 2. Depth-slice resistivity sections of the 3D model. Upper-left panel shows the shallowest section, and lower and right panels are deeper sections. Black dots indicate the MT sites. White dashed lines on the four shallowest sections are location of estimated faults. Letters C and R indicate typical conductive and resistive anomalies, respectively.

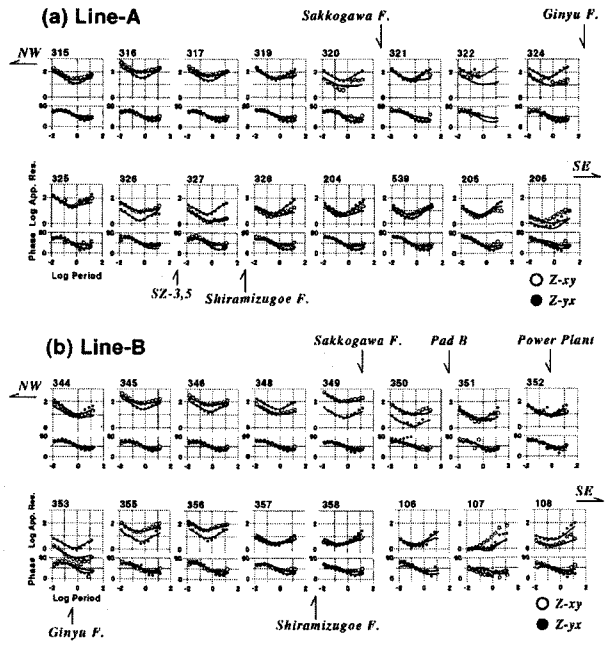

Fig. 3. Observed (circles) and computed (solid lines) apparent resistivities and phases of the sites on (a) Line-A and (b) Line-B. Open circles are *Zxy* and solid circles are Zyx. Static shifts are included in the computed apparent resistivity curves. Error bars are not shown in these panels, although they were used as the weight of each data in the inversion.

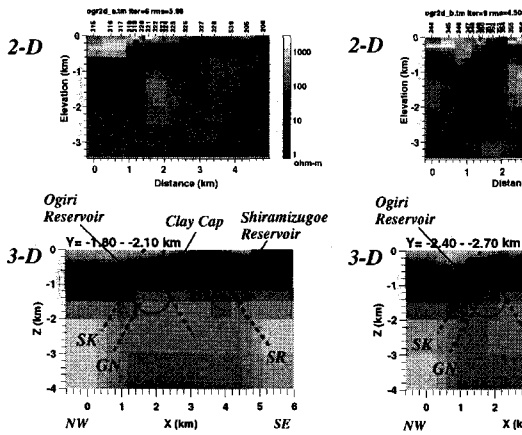

Fig. 4. Comparison of 2D and 3D models along (a) Line-A an (b) Line-B. The 2D models (upper panels) are from the inver sion of TM-mode MT data. The lower panels are vertical sec tions from the 3D model shown in Fig. 2. Thick dashed line are estimated faults. Large circles are estimated location o the production zones.

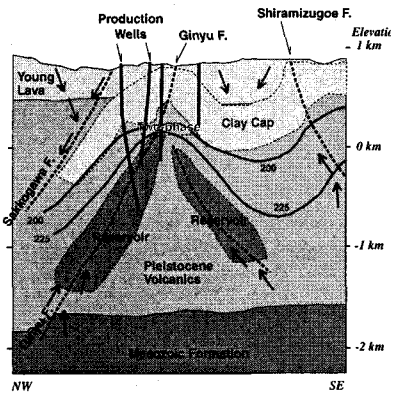

Fig. 5. A simplified geology section along NE-SW line around Lines A and B (repro duced from NEDO (2000)). Thick soli lines are several pilot and production wells. Contours with numbers are temperatur with values in degrees Celsius. Thick dashed lines indicate faults; thin dashe lines are estimated outlines of the reservoirs and clay cap. Arrows indicate estimated cold and hot water flows.

4. Interpretation of Pohang MT Data

Pohang geothermal field and MT data

We have conducted an MT survey in the Pohang low-enthalpy geothermal area, southeastern Korea, under a joint research project between the Korea Institute of Geoscience and Mineral Resources (KIGAM) and the Institute for Geo-Resources and Environment (GREEN), GSJ, AIST. The survey area is located in the north of Pohang City (Fig. 6) (Uchida et al. 2003). The main lineament structure in this area is the NNE-SSW trending Yangsan Fault, which runs west of the survey area. There are many other smaller lineaments that are parallel or in the conjugate directions with the Yangsan Fault. The major formations to the west of the Yangsan Fault are sedimentary and volcanic rocks in Cretaceous time, while the area to the east of the Yangsan Fault is mostly underlain by Tertiary sedimentary formations. There is a small basin structure around Heung-Hae Town, which is covered by Quaternary alluvium. The main target of the geothermal exploration and the MT survey was set in the southern side of the basin, where two minor lineaments in NNE-SSW and WNW-ESE directions intersect.

The field work was carried out in October-November 2002. MT stations were deployed on three survey lines that are arranged to cover the southern half of the Heung-Hae basin (Fig. 7). Lines 1 and 2 were set up to cross a minor NNE-SSW lineament. The number of stations was 33. As a first trial of the remote-reference MT in Korea, we deployed one remote station in Korea (R-1 in Fig. 6), which was 62 km from the Pohang survey area. Fortunately, we were also able to use other remote-reference data that were obtained in Kyushu, Japan, at the same time for another MT survey (R-2). By using these reference data, quality of the MT data was dramatically improved.

Fig. 8 compares MT impedances (apparent resistivities and phases) at Station 111 among single-site process, remote-reference process with Station R-1, and remote-reference process with Station R-2. In the single-site impedance curves, we can recognize near-field noises at frequencies from 0.1 Hz to 10 Hz, where the phase are almost zero (or -180 degrees) in both components of *xy* and *yx* and apparent resistivity curve of the *xy* component has a steep gradient of about 45 degrees. Most of these noises were removed by the remote-reference analysis with R-1, except that ambiguous noises remain between 0.1 Hz and 1 Hz. However, this portion was improved by the reference analysis with R-2.

Preliminary 2D and 3D interpretation

2D inversions were performed for two subsets of data for each survey line. One is for the TM mode data only, and the other is for both TM and TE mode data. Since there seem to be some static shifts in the TE data, it is difficult to match the TE apparent resistivity for Lines 1 and 2. Therefore, only TE phase, as well as TM apparent resistivity and phase, were used for the both-mode inversion for Lines 1 and 2. In this paper the models of Line-1 will be discussed.

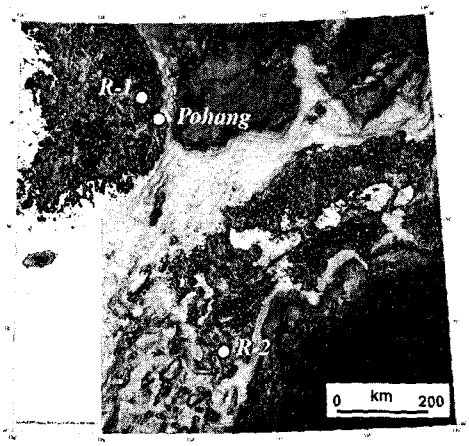

Fig. 6. Location of the Pohang area, remote reference stations in Korea (R-1) and Japa (R-2).

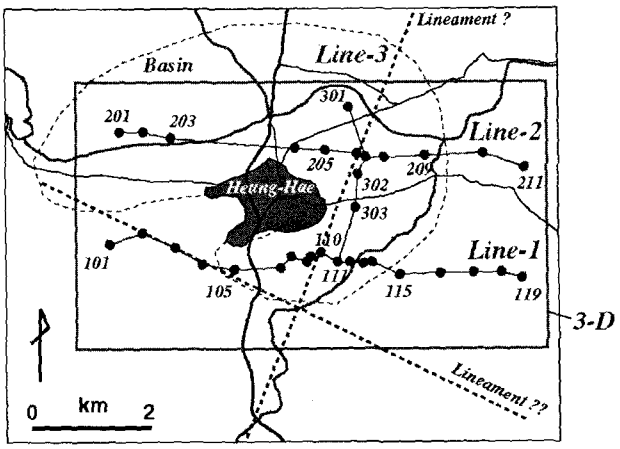

Fig. 7. Location of MT stations in the Pohang geothermal area southeastern Korea. Red circles are MT stations, the gra shaded area is Heung-Hae Town, black solid lines are roads blue solid lines are rivers, thick dashed lines are estimate lineaments, and the thin dashed line is the boundary of th basin structure. A gray rectangle indicates the zone of 3D in terpretation.

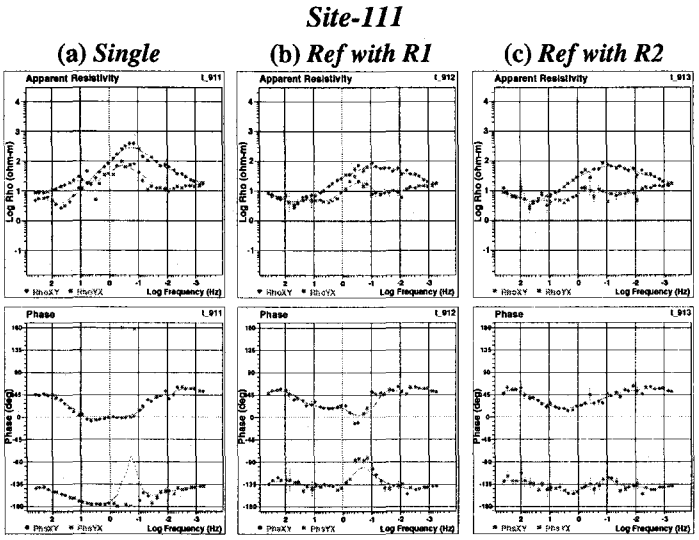

Fig. 8. Apparent resistivity and phase curves at Station 111 with (a) single-site process, (b) remote reference with R-1 in Korea, and (c) remote reference with R-2 in Japan. Circles (green) are the *xy*-component, and squares (orange) are *yx*-component. *x*-direction is true north..

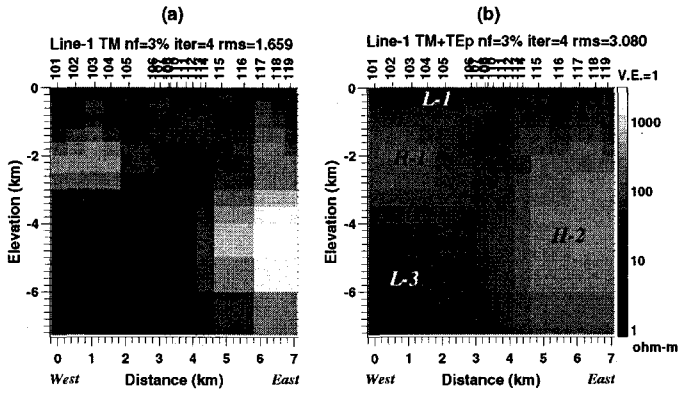

Fig. 9. 2D inverted models of Line-1: (a) TM mode data, and (b) TM and TE mode data. TE apparent resistivity data were not used in the latter. Typical anomalies are marked for the interpretation.

Fig. 9 shows 2D resistivity models of Line-1. There is a shallow low-resistivity layer with a thickness of approximately 200 – 400 m throughout the line. Its resistivity is approximately 10 ohm-m. This layer corresponds to the alluvium in the basin in the middle of the survey line and a shallow portion of the Tertiary formation at both ends of the line. Below is a thick high-resistivity layer of approximately 100 ohm-m. The lower limit of this resistive layer is 3 – 4 km in the western half of the line, while it is much deeper in the eastern half. Deep low-resistivity layer is recognized in the western half of the line. There seems to be a boundary at the middle of the line, which divides the deep resistivity structure between the west and east.

Fig. 10 shows depth-slice sections of the final 3D model. General features of the 3D resistivity model are consistent with the 2D models. However, the thickness of the high-resistivity second layer (H-1) became smaller than that of the 2D models. On the shallow sections, say above a depth of 400 m, slightly high-resistivity zones are recognized along the MT stations, while the zones between the lines seem to be in low-resistivity. This is because a part of resistivity values are explained by lateral resistivity change near the surface rather than the structure beneath the stations. As a result, these anomalies may distort the deep structures in the 3D model. This indicates that the irregular station arrangement for a 3D survey may create artifacts on the shallow sections.

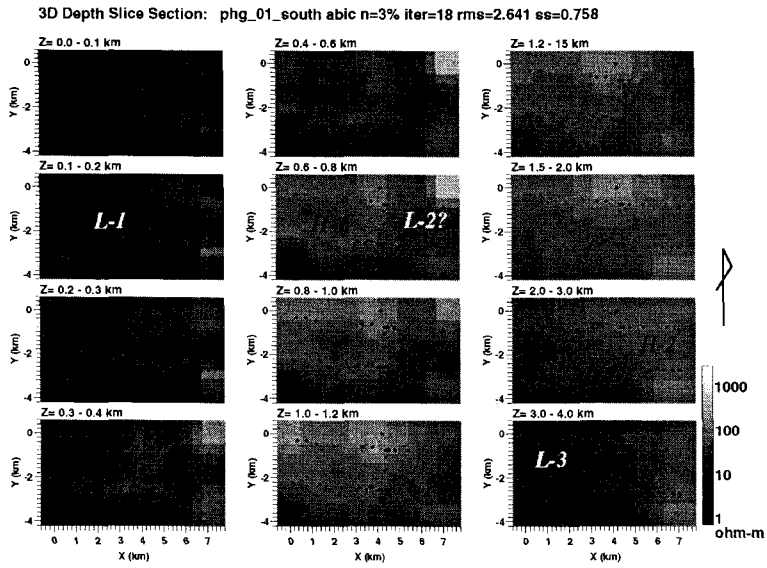

Fig. 10. Depth-slice resistivity sections of a preliminary 3D inverted model. Black dots are MT stations.

4. Conclusions

A 3D inversion technique based on the finite-difference forward modeling and the Gauss-Newton inversion scheme with smoothness regularization worked very well on a large volume MT field data obtained over the Ogiri and Shiramizugoe geothermal fields, southwestern Japan. Static shifts were solved simultaneously in the inversion. The optimum trade-off with regard to the roughness minimization and the static shift minimization was determined by a Bayesian criterion ABIC. 2D models beneath a few survey lines in Ogiri generated ambiguous structure at the boundary between the low-resistivity second layer and the high-resistivity third layer. It implies a limitation of the 2D interpretation. On the other hand, the 3D model seems to be more realistic for the entire resistivity model. Therefore, the 3D interpretation is essential for geothermal exploration, and more reliable 3D inversion technique is necessary for accurate imaging of deep resistivity structure.

On the other hand, a trial of 3D interpretation at the Pohang field is not successful yet. It is because the station coverage by three survey lines is not sufficient for 3D inversion. Further MT measurements are necessary in obtaining a reliable resistivity model of the area.

References

Goko, K., 2000, Structure and hydrology of the Ogiri field, West Kirishima geothermal area, Kyushu, Japan, Geothermics, v. 29, 127-149.

Mackie, R., Rodi, W., Watts, M. D., 2001, 3-D magnetotelluric inversion for resource exploration, Expanded Abstracts, Society of Exploration Geophysicists 71st Annual Meeting, 1501-1504.

NEDO, 2000, FY 1999 Report, Study on Geothermal Resources Exploration Techniques, Development of Technology for Reservoir Mass and Heat Flow Characterization, Electrical and Electromagnetic Monitoring (in Japanese).

Sasaki, Y., 1999, 3-D inversion of electrical and electromagnetic data on PC, Proceedings of 2nd International Symposium on Three-Dimensional Electromagnetics, 128-131.

Sasaki, Y., 2001, Three-dimensional inversion of static-shifted magnetotelluric data, Proceedings of 5th SEGJ International Symposium, 185-190.

Uchida, T., 1993, Smooth 2-D inversion for magnetotelluric data based on statistical criterion ABIC, Journal of Geomagnetism and Geoelectricity, v. 45, 841-858.

Uchida, T., Lee, T. J., Honda, M., Ashari, and Andan, A, 2002, 2-D and 3-D interpretation of magnetotelluric data in the Bajawa geothermal field, central Flores, Indonesia, Bulletin of Geological Survey of Japan, v. 53, 265-283.

Uchida, T., Lee, S. K., Mitsuhata, Y., Song, Y., 2003, MT interpretation in the Pohang geothermal field, Proceedings, 2003 Korea-Japan Joint Seminar on Geophysical Techniques for Geothermal Exploration and Subsurface Imaging, 32-45.